On the Structure of Aura and Co-occurrence Matrices for the Gibbs Texture Model*

Rosalind W. Picard
MIT Media Laboratory
20 Ames Street
Cambridge, MA 02139
picard@media.mit.edu

Ibrahim M. Elfadel
MIT Research Lab of Electronics
50 Vassar Street
Cambridge, MA 02139
elfadel@rle-vlsi.mit.edu

June 27, 1994

Abstract: The aura matrix of an image indicates how much of each graylevel is present in the neighborhood of each other graylevel and generalizes the popular texture analysis tool, the co-occurrence matrix. In this paper, we show that interesting structure appears in both the aura and co-occurrence matrices for textures which are synthesized from Gibbs random field models. We derive this structure by characterizing configurations of the distribution which are most likely to be synthesized when the Gibbs energy is minimized. This minimization is an important part of applications which use the Gibbs model within a Bayesian estimation framework for maximum *a posteriori* (MAP) estimation. In particular, we show that the aura matrix will become tridiagonal for an attractive auto-binomial field when suitable constraints exist on the histogram, neighborhood, and image sizes. Under the same constraints, but where the field is repulsive instead of attractive, the matrix will become anti-tridiagonal. The interpretation of this structure is especially significant for modeling textures with minimum energy configurations: zeros in the matrix prohibit certain colors from occurring next to each other, thus prohibiting large classes of textures from being formed.

Index Terms – co-occurrence matrix, energy minimization, pattern recognition, texture modeling, Gibbs/Markov random field

*This work was supported by the National Science Foundation and the Defense Advanced Research Projects Agency (DARPA) under Grant No. MIP-88-14612, the National Science Foundation under Grant No. IRI-8719920, the Rome Air Development Center (RADC) of the Air Force System Command and the Defense Advanced Research Projects Agency (DARPA) under contract No. F30602-89-C-0022.

1 Introduction

Since the equivalence between Markov and Gibbs random fields (GRF)'s was established by the Hammersley-Clifford theorem [1] there has been a great interest in using random field models for images and image texture patterns. A nice variety of textures have been shown to exist as samples of a Gibbs random field [2]. GRF's are also frequently incorporated into a Bayesian framework where, often by simulated annealing, a maximization is performed of an *a posteriori* probability [3]. In these cases and others where textures are being synthesized as samples of Gibbs models with low energy, it is helpful to know the kinds of patterns that are likely to be formed.

In a recent paper [4] we have shown that the Gibbs energy can be computed for a large class of GRF models by using a generalized form of graylevel co-occurrences that we call "aura measures." When organized in a matrix indexed by the graylevels, the aura measures form an "aura matrix" that is a generalization of the co-occurrence matrix, a popular texture analysis tool. We say that a "ground state aura matrix" is the aura matrix corresponding to the minimum energy pattern. The purpose of the present paper is to show that the structure of the ground state aura matrix can be determined algebraically for a large class of GRF texture models. We provide a detailed analysis of the auto-binomial GRF case and indicate how the methodology can be applied to the case of another popular texture model, the Potts model.

The results described in this paper are significant because of the following reasons:

1. Knowing the structure of the ground state aura matrix helps characterize the minimum energy pattern and when it is attained.

2. These results indicate, apparently for the first time, a relationship between a texture synthesis model and its co-occurrence matrix. Identifying properties of a texture which correspond to structure in co-occurrence matrices has been an important pursuit [5].

3. Most importantly, we show for the first time that the ground state aura matrix structure implies strong restrictions about which classes of patterns can and cannot be generated as minimum energy configurations of the auto-binomial GRF.

The paper is organized as follows. Section 2 contains the notation, assumptions, and basic definitions of the paper. It is also motivational in that it describes the basic experimental discovery that has led to the theory developed in this paper. Background for the aura framework is provided in Section 2.3. Sections 3–6 are the mathematical groundwork of the paper. Based on Birkhoff's theorem about the convex hull of permutation matrices, we show why what has been observed experimentally is theoretically bound to happen, given the assumptions and the constraints of the problem. We have assigned the proofs to a set of appendices that can be consulted as desired; our results can be understood without reading these appendices. In Section 7, we comment on some of the applications and implications of the results obtained in this paper. Finally, the last section is devoted to a summary of our findings.

2 Background

2.1 Notation and assumptions

Let an image be represented by a finite rectangular $M \times N$ lattice $\mathcal{S}$ with a neighborhood structure $\mathbf{N} = \{\mathcal{N}_s, s \in \mathcal{S}\}$, where $\mathcal{N}_s \subseteq \mathcal{S}$ is the set of neighbors of the site $s \in \mathcal{S}$. Every site has a graylevel value $x_s \in \Lambda = \{0, 1, \ldots, n-1\}$. Let $\mathbf{x}$ be the vector $[x_s, 1 \leq s \leq |\mathcal{S}|]$ of site graylevel values and Ω be

the set of all configurations taken by $\mathbf{x}$. A neighborhood structure is said to be *symmetric* if $\forall s, r \in \mathcal{S}$, $s \in \mathcal{N}_r$ if and only if $r \in \mathcal{N}_s$. The set of all sites with graylevel g is $\mathcal{S}_g = \{s \in \mathcal{S} | x_s = g\}$, $\forall g \in \Lambda$. The vector of graylevel values is $\mathbf{g} = [0, 1, \ldots, n-1]^T$.

The basic methodology for GRF texture synthesis is the following. For the finite periodic lattice $\mathcal{S}$, with the symmetric neighborhood structure $\{\mathcal{N}_s, s \in \mathcal{S}\}$, we define the local two-site interaction potentials between neighboring pixels, $V_{sr}(x_s, x_r), r \in \mathcal{N}_s$, and the Gibbs energy

$$E(\mathbf{x}) = \sum_{s \in \mathcal{S}} \sum_{r \in \mathcal{N}_s} V_{sr}(x_s, x_r). \tag{1}$$

To the Gibbs energy, thus defined, we can assign a random field whose probability distribution is given by

$$P(\mathbf{x}) = \frac{1}{Z} \exp(-\frac{1}{T} E(\mathbf{x})), \tag{2}$$

where T is the "temperature" of the field and Z is a positive normalizing constant, also known in the physics literature as a partition function. The relationship between the above joint probability distribution and Markov random fields is now part of the mainstream culture in image modeling [3], and we will not dwell on it. However, it is important for the subsequent development of the theory to make explicit our assumptions.

1. **Homogeneity, isotropy, symmetry:** As is typical in the GRF literature we assume a *homogeneous* random field so that the model is shift-invariant. In Section 3 we start our analysis by assuming that the field is *isotropic* so that the interaction potentials V_{sr} are all the same and equal to V. Of course, most natural textures have *anisotropy*. The generalization of our results to the anisotropic case is addressed in Section 6. Finally, a constraint imposed by the homogeneity of the GRF is that the neighborhood structure must be symmetric.

2. **Histograms, image and neighborhood sizes:** Without any histogram constraints the optimum state of the isotropic GRF may have a trivial patternless solution. Though real textures can have any histogram, we assume that the histogram is constrained to be uniform throughout the pattern formation. Thus, $|\mathcal{S}_g| = NM/n = \gamma$, $\forall g \in \Lambda$. This is equivalent to the maximum entropy prior when nothing is known about the initial distribution. Monte Carlo synthesis methods such as the Metropolis exchange algorithm implicitly constrain the histogram to be equal to its initial value. Note that strictly speaking, the histogram constraint destroys Markovianity; thus, it is a misnomer to call the constrained Gibbs random field a Markov random field.

   We further assume that the image size is "large" compared to both the neighborhood size and number of graylevels. This assumption can be formalized by letting the lattice dimension $|\mathcal{S}| = MN \to \infty$ while $|\mathcal{N}_s| = \nu$ and n take typical image processing values $4 \leq \nu \leq 20$ and $2 \leq n \leq 256$. Typical neighborhoods for GRF's of orders 1-4 are shown in Figure 1 (a). In practice, images of size 64×64 are large enough to demonstrate the results derived in this paper.

3. **Lattice connectivity and periodic boundary:** We represent an image as a lattice with each pixel corresponding to a node. When the image is modified only the values at lattice nodes may change. This representation implicitly assumes a connected lattice. For simplicity of notation we also assume a periodic boundary.

2.2 Texture formation: the auto-binomial model

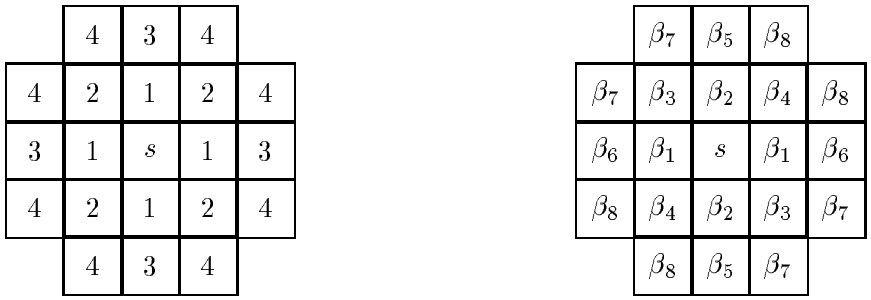

(a) (b)

Figure 1: (a) Neighbors of the site s for model orders 1-4. The neighborhood of order p contains all points with labels $\leq p$. (b) The auto-binomial bonding parameter β_k corresponding to each neighbor.

In this section we consider the auto-binomial Gibbs model first studied for textures in [6], and shown there to be capable of synthesizing a large variety of patterns. The homogeneous model has the pairwise interaction potential $V_{sr}(x_s, x_r) = -\beta_r x_s x_r$, where β_r is a bonding parameter which weights the neighbors as shown in Figure 1 (b).

The use of this model to synthesize textures is illustrated in Figure 2 where twelve 64×64 samples with $n = 8$ are shown for three different sets of parameters. Within a column all the samples have the same set of parameters. Each was also synthesized at a constant temperature, $T = 1$ (no annealing; this is the case for all the texture samples shown in this paper). The rows correspond to samples of a GRF after the 0, 10, 100, and 1000 iterations of synthesis using the Metropolis exchange algorithm as was done in [2].

The first row shows the effect of one iteration of the synthesis on an initial uniform random image. In the second row are textures which were said to have "converged" according to the criteria of [2, 6, 7]. Patterns synthesized with about 10-15 iterations, like those in the second row, have been shown to correspond nicely to stochastic natural texture patterns. It has been assumed that the values of the GRF bonding parameters correspond to textures formed at this stage of the synthesis process.

The reason we show this example is to indicate that although the patterns are changing quite slowly, after 100 and 1000 iterations (rows three and four) the patterns are perceptually different. That is, in each column, one set of parameters is generating more than one type of texture pattern. The changes in each column indicate that the energy for the given parameters is still being minimized. Natural questions which arise then are, "what will the minimum energy pattern look like?" and "how will one know when it is reached?" In this paper, we will show how the aura matrix is useful for answering these questions.

2.3 Aura measures, aura matrices: definitions and properties

The aura measure indicates "how much" of a general subset is present in the neighborhood of another subset. Although the measure is general, in this paper the subsets are the $\mathcal{S}_g$'s, i.e., sets of sites having the same graylevel. The aura measure has been formally defined as follows [8]:

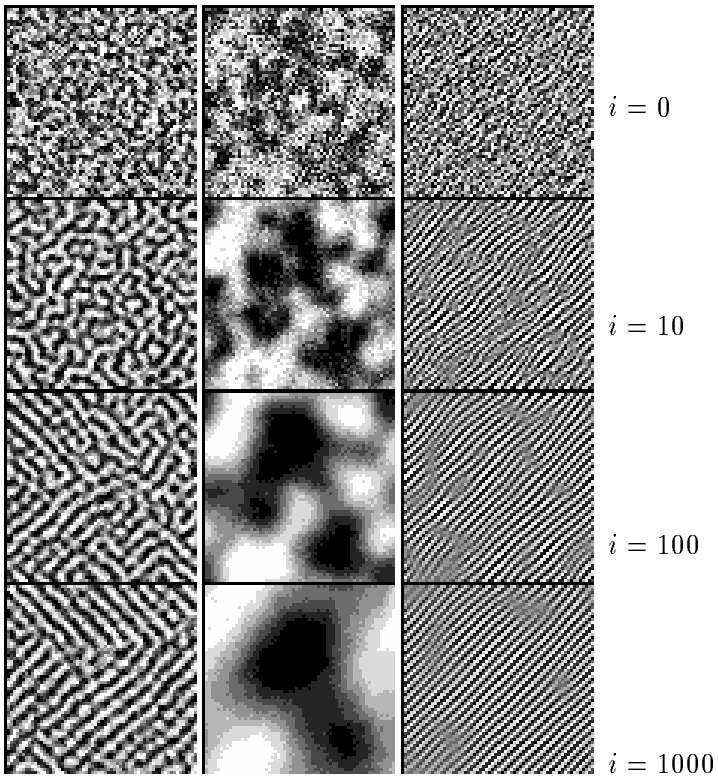

Figure 2: In each column, four 64×64 samples of an MRF are shown. The parameters in (a) are $\beta_1 = \beta_2 = \beta_3 = \beta_4 = 0.2$, and $\beta_5 = \beta_6 = \beta_7 = \beta_8 = -0.1$, (b) $\beta = 0.5$, and (c) $\beta_1 = \beta_2 = \beta_3 = \beta_5 = \beta_6 = -0.4$, $\beta_4 = 0.4$.

Definition 1 *Let A, B be two subsets on the lattice and let $\mathcal{N}_s$ be a neighborhood structuring element. The aura measure, denoted by $m(A, B)$, is defined by*

$$m(A, B) = \sum_{s \in A} |\mathcal{N}_s \cap B|. \tag{3}$$

Now consider the case where we have a collection of subsets that form a partition of the lattice. Then we can define the aura measures of these subsets with respect to each other. The following definition is adopted from [9]:

Definition 2 *Let $S_i \subseteq \mathcal{S}$, $i = 0, 1, \ldots, n-1$, $\bigcup_{i=0}^{n-1} S_i = \mathcal{S}$ and $S_i \cap S_j = \emptyset$ unless $i = j$. Then the aura matrix, $\mathbf{A}$, is the $n \times n$ integer matrix defined by $\mathbf{A} = [a_{ij}]$ where $a_{ij} = m(S_i, S_j)$, $0 \leq i, j \leq n-1$.*

For any two graylevel sets $\mathcal{S}_g, \mathcal{S}_{g'}$, we use the shorter notation $m(g, g') = m(\mathcal{S}_g, \mathcal{S}_{g'})$. The normalized aura matrix, $\mathbf{M}$, is defined by $\mathbf{M} = \frac{1}{\gamma\nu}\mathbf{A}$, and referred to as the *miscibility matrix*. The elements of $\mathbf{M}$ will be denoted by $\mathbf{m}(g, g')$.

When the neighborhood structure is symmetric, the aura matrix, and therefore the miscibility matrix is symmetric. Moreover, because of the uniform histogram constraint, the miscibility matrix is doubly

stochastic[1]. These statements, along with many other properties of the aura matrix and aura measures are proved in [8]. In addition to these properties, the constraints of the lattice geometry yield the following:

1. **Aura matrix irreducibility:** Because the lattice is connected, one can reach any graylevel set from any other graylevel set. Equivalently, from any row i of the aura matrix, there is a path of non-zero elements, a_{ik}, a_{kj}, a_{jl}, etc., which eventually reaches all the rows. This is equivalent to the constraint that the aura matrix be *irreducible*. An example of an irreducible matrix is one that has $a_{ij} \neq 0$ for $|i-j| = 1$; an example of a reducible matrix is one that is block diagonal.

2. **Constraints on boundary length:** On the connected lattice with more than one graylevel there will be boundaries between the different graylevels, g, g'. A length related to $m(g, g')$ can be associated with these boundaries. Upper and lower bounds for $m(g, g')$ can be determined easily in some cases.

   Example 1 *Consider the binary case with four nearest neighbors on an $M \times N$ lattice. The minimum boundary occurs when the graylevels (or in general, "colors") divide into two regions. The boundary between the two regions will be as straight as possible, attaining in the limit a minimum length of $m(0,1) = 2\min(M,N)$. Note that if we did not assume a periodic lattice, then the minimum length would be $m(0,1) = \min(M,N)$ since the regions would no longer share an edge along the lattice boundary. Similarly, the maximum boundary length occurs when two colors form a checkerboard; it has length $2NM$.*

One of the most interesting features of the aura measures is that they reveal a linear structure behind the Gibbs energy minimization. For the case of the isotropic, homogeneous, pairwise interaction model, it has been shown that the Gibbs energy can be rewritten as a linear combination of aura measures [4],

$$E(\mathbf{x}) = \sum_{g,g' \in \Lambda} V(g, g') m(g, g'). \tag{4}$$

A generalization of this result to an anisotropic field was given in [9]. The aura matrix irreducibility and the bounds on boundary length can also be written as linear constraints on the aura measures. These constraints along with the linear form of the Gibbs energy as a cost function constitute a linear program with the aura measures as variables. Theoretically, this program can be solved to find the aura measures. The approach adopted here is however different as is explained in the subsequent sections.

3 Structure of the auto-binomial aura matrix: isotropic case

This section begins the mathematical groundwork of the paper. From now on we concentrate on characterizing the textures that minimize the Gibbs energy.

3.1 Formulation

Using the linear aura formulation for the Gibbs energy, the cost function being minimized for an isotropic, homogeneous, auto-binomial GRF where $V(g, g') = -\beta g g'$, is

$$\min_{\mathbf{x} \in \mathbf{\Omega}} -\beta \sum_{g,g' \in \Lambda} g g' m(g, g') \tag{5}$$

[1] A *doubly stochastic* matrix is one where all elements are nonnegative and where every row and column sums to 1.

which in terms of the aura matrix can be written as

$$\max_{\mathbf{x}\in\mathbf{\Omega}} \beta \mathbf{g}^T \mathbf{A} \mathbf{g}. \tag{6}$$

The maximization is over the set of image configurations; these configurations determine the values of the aura measures, $m(g, g')$. Solving the above problem is equivalent to solving

$$\max_{\mathbf{x}\in\mathbf{\Omega}} \beta \mathbf{g}^T \mathbf{M} \mathbf{g}, \tag{7}$$

since scaling the objective function does not change the solution. The intent of this paper is to show what kind of matrix (and hence, pattern) structure will occur when the optimization is solved.

3.2 Decomposition into permutations

The following theorem by Birkhoff is the key new insight used to derive the structure in the aura matrix.

Theorem 1 *Every doubly stochastic matrix is a convex combination of permutation* [2] *matrices.*

Proof: A proof appears in [10]. ■

Theorem 1 means that $\mathbf{M}$ can be decomposed as

$$\mathbf{M} = \sum_{\sigma\in\mathcal{P}_n} \alpha_\sigma \mathbf{P}_\sigma, \tag{8}$$

where $\mathbf{P}_\sigma \in \Re^{n\times n}$ is the permutation matrix corresponding to the permutation $\sigma \in \mathcal{P}_n$, the group of all permutations of the set $\Lambda = \{0, 1, \ldots, n-1\}$, and where the α_σ's satisfy the constraints

$$\sum_{\sigma\in\mathcal{P}_n} \alpha_\sigma = 1,\ \alpha_\sigma \geq 0,\ \forall\sigma \in \mathcal{P}_n.$$

Combining (8) with (7) gives

$$\begin{aligned} \max_{\mathbf{x}\in\mathbf{\Omega}} \quad & \beta \sum_{\sigma\in\mathcal{P}_n} \alpha_\sigma \mathbf{g}^T \mathbf{P}_\sigma \mathbf{g} \\ \text{subject to} \quad & \sum_{\sigma\in\mathcal{P}_n} \alpha_\sigma = 1,\ \alpha_\sigma \geq 0,\ \forall\sigma \in \mathcal{P}_n. \end{aligned} \tag{9}$$

We will focus on solving the problem in (9) subject to assumptions stated in Section 2.

3.3 Aura matrix structure: example

Before proceeding with our arguments it is helpful to consider an example of the aura matrix structure. Returning to Figure 2, we compute the aura matrices for each of the attractive isotropic patterns in column (b).

Suppose the elements along each diagonal of $\mathbf{M}$ are summed,

$$M_\delta = \sum_{i-j=\delta} \mathbf{m}(i, j), \quad \delta = -(n-1), \ldots, 0, \ldots, n-1.$$

[2] A brief review of the basic usage of permutations is provided in Appendix A.

If M_δ vs. δ were plotted at different energy values, then it would be observed to "sharpen" around $\delta = 0$ as the energy is decreased. This corresponds to the matrices becoming more and more diagonal; Figure 3 shows the M_δ for the aura matrices of Figure 2 (b).

Is this behavior typical? The arguments which follow indicate "yes." We will show that for the isotropic attractive case, under suitable assumptions, this sharpening will always occur. For the isotropic repulsive case it will also occur, but along the anti-diagonal. For anisotropic cases the behavior will be a combination of these "sharpening" effects. These three case will be dealt with in detail in the next three sections.

4 Structure of the auto-binomial aura matrix: attractive case

For the attractive case, $\beta > 0$, we want to characterize the σ's (permutations) which maximize the sum of nonnegative numbers,

$$\sum_{\sigma \in \mathcal{P}_n} \alpha_\sigma \mathbf{g}^T \mathbf{P}_\sigma \mathbf{g}, \tag{10}$$

subject to the constraints and assumptions already stated. The resulting set of $\mathbf{P}_\sigma$'s which maximizes (10) will provide the structure of the "ground state" aura matrix. In Sections 4.1-4.2 this set of permutations is characterized, yielding the key insights into the matrix structure. Section 4.3 discusses approximations on the coefficients, α_σ, corresponding to these permutations.

4.1 "Best" solution is infeasible

Since $\mathbf{P}_\sigma$ is a permutation matrix it is orthogonal and preserves the norm, i.e., $\|\mathbf{P}_\sigma \mathbf{g}\| = \|\mathbf{g}\|$. Hence, the dot product $\mathbf{g}^T \mathbf{P}_\sigma \mathbf{g}$ is equal to $\|\mathbf{g}\|^2 \cos\theta_\sigma$ where θ_σ is the angle between $\mathbf{g}$ and $\mathbf{P}_\sigma \mathbf{g}$. Observe that the maximum of this dot product occurs when $\cos\theta_\sigma = 1$, corresponding to $\mathbf{P}_\sigma = \mathbf{I}$, the identity matrix. Using only the identity permutation, σ_I, there is a trivial solution which maximizes (10): $\aleph = \{\alpha_\sigma \mid \alpha_\sigma = 1 \text{ for } \sigma = \sigma_I, \text{ and } \alpha_\sigma = 0 \text{ for all other } \sigma \in \mathcal{P}_n\}$.

However, the trivial solution is infeasible. By assumption of a connected lattice, $\mathbf{M}$ must be irreducible; thus, $\mathbf{M}$ cannot be diagonal, and consequently, it cannot be constructed from only a weighted identity matrix. If it were feasible the "sharpening process" would yield a bandwidth function, M_δ, that is just an impulse at $\delta = 0$.

4.2 "Next best" solution

Now we characterize the permutations which give the "next best" maximum of the objective function. With a sufficiently large lattice, these do provide a feasible solution.

Note that maximizing (10) is the same as minimizing

$$\mu_{\mathbf{g}} = \mathbf{g}^T \mathbf{g} - \sum_{\sigma \in \mathcal{P}_n} \alpha_\sigma \mathbf{g}^T \mathbf{P}_\sigma \mathbf{g}. \tag{11}$$

which can also be written as

$$\mu_{\mathbf{g}} = \sum_{\sigma \in \mathcal{P}_n} \alpha_\sigma \left(\mathbf{g}^T \mathbf{g} - \mathbf{g}^T \mathbf{P}_\sigma \mathbf{g} \right) = \sum_{\sigma \in \mathcal{P}_n} \alpha_\sigma \mu(\sigma), \tag{12}$$

because $\sum_{\sigma \in \mathcal{P}_n} \alpha_\sigma = 1$.

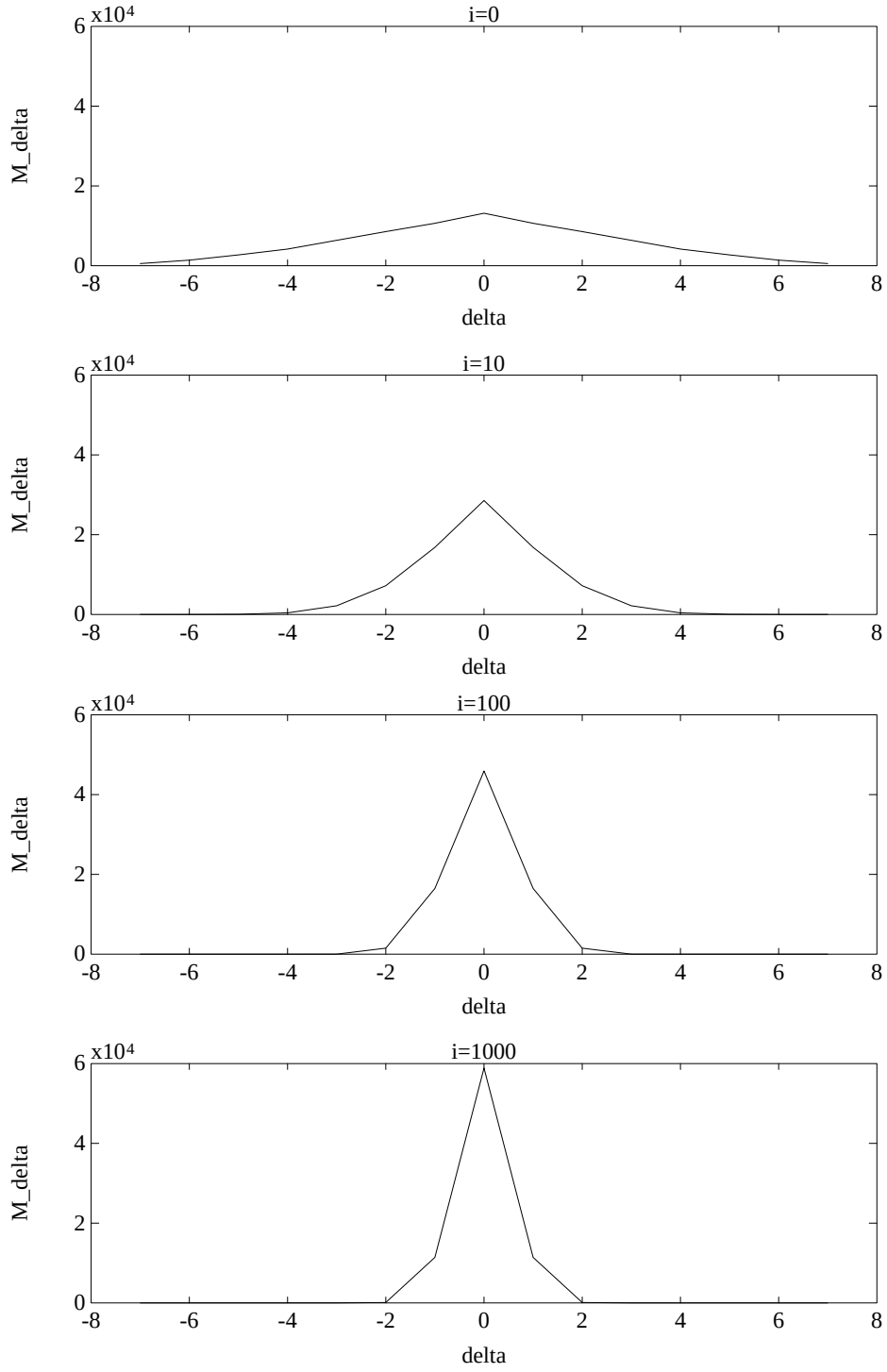

Figure 3: Sharpening of the bandwidth function, M_δ, for the four textures in Figure 2 (b).

It suffices now to find the "next best" maximum of (10) by choosing $\mathbf{P}_\sigma \neq \mathbf{I}$ that minimizes the "mismatch,"

$$\mu(\sigma) = \mathbf{g}^T\mathbf{g} - \mathbf{g}^T\mathbf{P}_\sigma\mathbf{g}. \tag{13}$$

Intuitively we must find the permutations which make $\mathbf{P}_\sigma\mathbf{g}$ as close as possible to $\mathbf{g}$ but not equal to it. A standard result from algebra [11] states that every permutation can be written as a product of its disjoint cycles $\sigma = \sigma_1\sigma_2\ldots\sigma_k$ [3].

Let Λ_j denote the set of elements in Λ which the cycle σ_j permutes. Clearly we have $\bigcup_{1\leq j\leq k}\Lambda_j = \Lambda$ and since the cycles are disjoint, the Λ_j's form a partition of Λ. Observe that if $q \in \Lambda_j$, then $\sigma_j(q) \in \Lambda_j$. Also, $\forall q \notin \Lambda_j$, we have $\sigma_j(q) = q$.

Let the length of a cycle σ_j be the number of elements of Λ_j and denote this length by l_j. Denote the set of adjacent transpositions (cycles which contain only two adjacent elements from Λ) by $\mathcal{P}_\tau \subset \mathcal{P}_n$. Note that for all $n-1$ permutations $\sigma \in \mathcal{P}_\tau$, the corresponding permutation matrix $\mathbf{P}_\sigma$ is tridiagonal.

Example 2 *Consider the case where $n = 4$. Then the following three permutation matrices correspond to $\sigma \in \mathcal{P}_\tau$:*

$$\begin{bmatrix} 0 & 1 & 0 & 0 \\ 1 & 0 & 0 & 0 \\ 0 & 0 & 1 & 0 \\ 0 & 0 & 0 & 1 \end{bmatrix} \qquad \begin{bmatrix} 1 & 0 & 0 & 0 \\ 0 & 0 & 1 & 0 \\ 0 & 1 & 0 & 0 \\ 0 & 0 & 0 & 1 \end{bmatrix} \qquad \begin{bmatrix} 1 & 0 & 0 & 0 \\ 0 & 1 & 0 & 0 \\ 0 & 0 & 0 & 1 \\ 0 & 0 & 1 & 0 \end{bmatrix}.$$

The following proposition, proved in Appendix B, is instrumental to our arguments.

Proposition 1 *Let σ be a permutation different from the identity. Write the decomposition of σ into disjoint cycles as $\tau_1\ldots\tau_t\sigma_1\ldots\sigma_k$, where $\tau_1,\ldots,\tau_t$ represent the disjoint cycles which are adjacent transpositions. Denote the lengths of $\sigma_1,\ldots,\sigma_k$ by $l_1,\ldots,l_k \geq 2$, respectively. Then*

$$\mu(\sigma) \geq t + \sum_{j=1}^{k} l_j.$$

From the above proposition, one can easily prove

Corollary 1 *Let $\sigma \in \mathcal{P}_n$ be an arbitrary permutation. Then $\mu(\sigma) = 1$ if and only if σ is an adjacent transposition.*

It follows that the adjacent transposition has the minimum mismatch of all permutations except the identity permutation. Therefore the desired "next best" maximum of (10) is given by the permutation matrices $\mathbf{P}_\sigma, \sigma \in \mathcal{P}_\tau$. Consequently, the permutations of $\mathcal{P}_\tau^* = \mathcal{P}_\tau \cup \{\mathbf{I}\}$ both maximize (9) and satisfy all the constraints.

We have finished characterizing the permutations we will need for our main results. In the next section, we discuss the role of the coefficients, α_σ, used in the convex combination of the permutations. These coefficients are related to the minimum boundary lengths which can occur between the different sets of graylevels in the pattern.

[3] A brief review of cycles is provided in Appendix A.

4.3 Minimum boundary approximations

Let us consider simplifying the optimization problem in (9) by keeping only the elements of $\mathcal{P}_n$ which are equal to the identity permutation or an adjacent transposition. Let these two cases be represented by $w_0 = \mathbf{g}^T\mathbf{I}\mathbf{g}$, and $w_1 = \mathbf{g}^T\mathbf{P}_\sigma\mathbf{g}$, $\sigma \in \mathcal{P}_\tau$. Because σ is an adjacent transposition, by Corollary 1, $w_1 = w_0 - 1$. Let $\bar{\alpha} = [\alpha_i]^T$. We now have

$$\begin{aligned} \max_{\bar{\alpha}} \quad & \alpha_0 w_0 + \left(\sum_{i=1}^{n-1} \alpha_i\right)(w_0 - 1) \\ \text{subject to} \quad & \alpha_0, \alpha_i > 0 \\ & \alpha_0 + \sum_{i=1}^{n-1} \alpha_i = 1. \end{aligned} \tag{14}$$

The case $n = 2$ can be easily treated – it becomes a maximization of α_0, subject to the constraints $\alpha_0 = 1 - \alpha_1$ and $\alpha_1 > 0$. Intuitively, this corresponds to maximizing the elements along the diagonal of the aura matrix, but not allowing it to become a diagonal matrix. The off diagonal elements decrease to the lower bound on $\mathbf{m}(0,1)$ found in Example 1. In general, however, solving for these lower bounds can be very difficult. We will briefly discuss the problem with $n > 2$, and then examine some helpful approximations on the α_i.

Consider the general case $n > 2$. Note that all the α_i, $1 \le i \le n-1$ are weighted by the same constant. When the Monte Carlo optimization algorithm rearranges the pixels to maximize a weighted sum, it will tend to contribute more to the terms having higher weights. Since the α_i have the same weights, and since we are assuming a uniform distribution of graylevels, on average the algorithm will contribute uniformly to α_i, $1 \le i \le n-1$. Characterizing α_0 and the expected value of the others, $\hat{\alpha} = \mathrm{E}(\alpha_i)$, the problem can be rewritten as,

$$\begin{aligned} \max_{\bar{\alpha}} \quad & [\alpha_0 + (n-1)\hat{\alpha}]w_0 - (n-1)\hat{\alpha} \\ \text{subject to} \quad & \alpha_0, \hat{\alpha} > 0 \\ & \alpha_0 + (n-1)\hat{\alpha} = 1. \end{aligned} \tag{15}$$

By substituting the second constraint into the objective function, it is evident that the problem is solved by minimizing $\hat{\alpha}$. Since $\hat{\alpha}$ corresponds to the values off the diagonal, its minimization is achieved by setting it equal to the lower bound of $\mathbf{m}(0,1)$.

From miscibility analysis [4] we know that the "mixing" between colors 0 and 1, $m(0,1) = \gamma\nu\mathbf{m}(0,1)$, is bounded below by the minimum boundary length between the two graylevels. Intuitively, the only reason we would not be able to find α_i which solve (15) is if there are not enough elements of graylevel 1 to surround the set of graylevel 0. If there are not enough 1's, then it must be true that $m(0,i) > 0$ for some other graylevel $i > 1$. If this were the case then the matrix would not be tridiagonal.

Since finding precise lower bounds on the boundary lengths between different graylevels is quite difficult in general, we consider some reasonable approximations that indicate where the aura matrix structure results will hold.

In the plane, the minimum boundary around a set $\mathcal{S}_g$ of size γ is approximately the circumference of a circle of area γ. The circumference can be roughly approximated by the aura measures for the $p = 1, 2$ order neighborhoods. Let $\gamma = \pi r^2$ so that $r = \sqrt{\gamma/\pi}$; then the circumference is $c = 2\sqrt{\gamma\pi}$. For approximately $\gamma > c$, i.e., $\gamma > 4\pi$, the set $\mathcal{S}_g$ can be surrounded by the set $\mathcal{S}_{g'}$.

For higher order GRF's these approximations also need to incorporate the width, ω, of the neighborhood. (The width considered here is a nonlinear function of the neighborhood; for p=1,2 the width

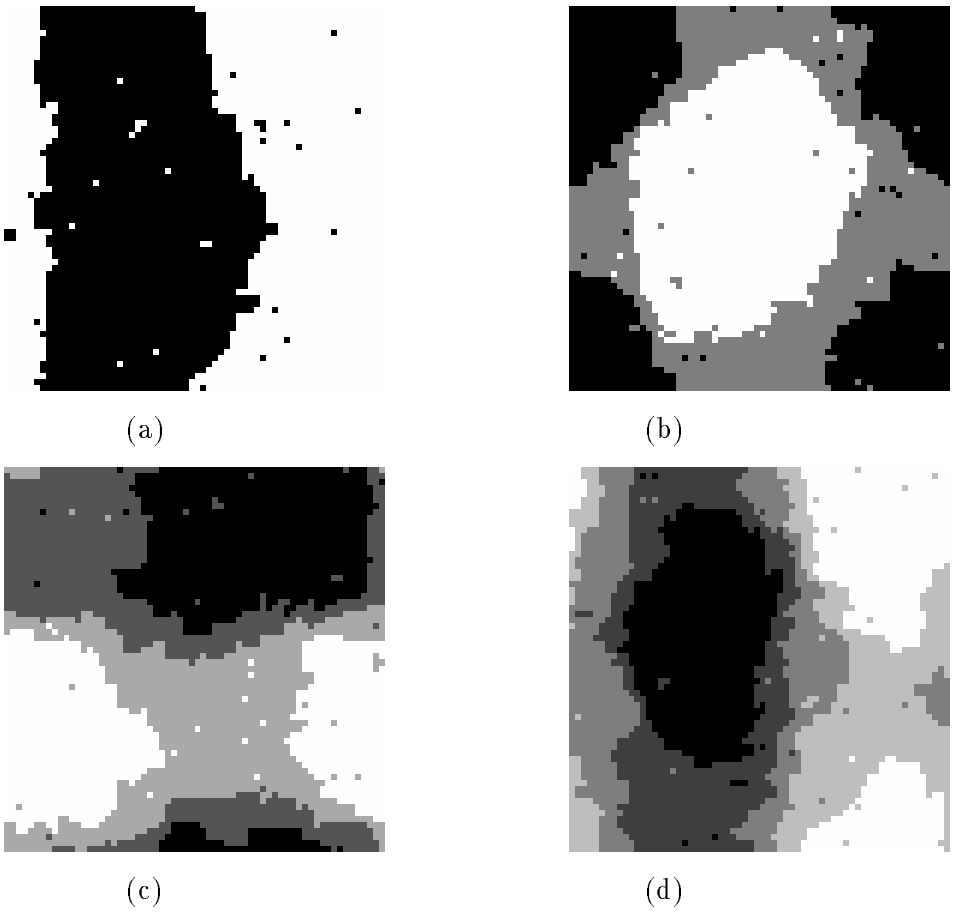

Figure 4: Examples of near-minimum-energy patterns for first-order MRF's with postive isotropic bonding parameters. Images (a)-(d) correspond to 2-5 graylevels respectively. Each image is 64×64.

---

is 1; for p=3,4 the width is 2, etc.) If the measure is formed over a wider neighborhood, and if it is to only contain one color, then there needs to be enough of that color to surround the set of 0's throughout the width of that neighborhood. Thus one would need approximately $\gamma > 4\pi\omega$. For $\omega = 1$ the 64×64 image is sufficiently large for a standard 256 graylevel image to develop the tridiagonal structure.

4.4 Minimum boundary configurations

As mentioned, the problem of characterizing minimum boundary configurations is very difficult. With the assumptions we made at the start, and when $\gamma = NM/n$ is sufficiently large, then there are orderly configurations for the colors which always permit the tridiagonal structure. Examples of patterns which nearly have these minimum boundaries are shown in Figure 4.

The above arguments allow us to state the following key result for the structure of the attractive isotropic auto-binomial GRF aura matrix:

Proposition 2 *For NM/n large enough compared with $4\pi\omega$ the ground state aura matrix of the attractive isotropic auto-binomial GRF is tridiagonal.*

Given the structure of the ground state aura matrix, its trace can also be characterized.

Corollary 2 *The trace of the ground state aura matrix of the attractive isotropic auto-binomial GRF will increase linearly with respect to the number of graylevels. Let α_0 be the weight of the identity permutation. Then,*

$$\sum_{i=0}^{n-1} m(i,i) = \gamma\nu \sum_{i=0}^{n-1} \mathbf{m}(i,i) = \gamma\nu[n + (2\alpha_0 - 2)].$$

The proof of the corollary is in Appendix C. The trace for the ground state miscibility matrix is bounded above by n, and could only equal n if $\alpha_0 = 1$, i.e., if the aura matrix becomes reducible.

If the relative bounds of Proposition 2 are not satisfied then the new structure can be predicted by continuing the analysis method set forth in this paper. For example, the "next best" set of permutations are those in the set $\mathcal{P}_n - \mathcal{P}_\tau^*$ with minimum mismatch. For $n \geq 4$ this would be the permutations comprised of two adjacent transpositions, i.e., $\mu(\sigma) = 2$. Use of these would still preserve the tridiagonal structure. The structure will increase to penta-diagonal at the point where cycles of length 3 are required, and so forth.

5 Structure of the auto-binomial aura matrix: repulsive case

In this section where $\beta < 0$, we will show that there is a nice symmetry which enables this same analysis to be applied "at the other end", finding the permutations with *maximum* mismatch. These also have the property of maximizing miscibilities, hence maximizing boundary lengths [4].

5.1 Energy in terms of the reversing permutation

Now we want to characterize the σ's which *minimize* the sum of positive numbers,

$$\sum_{\sigma \in \mathcal{P}_n} \alpha_\sigma \mathbf{g}^T \mathbf{P}_\sigma \mathbf{g}, \tag{16}$$

subject to the constraints and assumptions already stated. For $n = 2$, the minimum value 0 is reached by setting

$$\mathbf{P}_\sigma = \begin{bmatrix} 0 & 1 \\ 1 & 0 \end{bmatrix}.$$

Observe that for $n > 2$ the minimum is strictly positive; both $\mathbf{g}$ and $\mathbf{P}_\sigma\mathbf{g}$ are in the positive orthant of $\Re^n$. Observe also that minimizing the above sum is equivalent to maximizing the mismatch, $\mu(\sigma)$, of (13), i.e., finding the vector "farthest" from $\mathbf{g}$.

Let ρ be the permutation that reverses the order of the components of the vector $\mathbf{g}$. For $i \in \Lambda$, we have $\rho(i) = n - 1 - i$. We will show now that the mismatch of the reversing permutation $\mu(\rho)$ is an upper bound on $\mu(\sigma)$, $\sigma \in \mathcal{P}_n$. We will also show that $\mu(\rho\tau)$, where τ is an adjacent transposition, is an upper bound on $\mu(\sigma)$, $\sigma \in \mathcal{P}_n - \{\rho\}$.

In order to accomplish this we consider the difference,

$$\Delta(\sigma) = \mu(\rho) - \mu(\rho\sigma) = \sum_{i=0}^{n-1} i[\rho\sigma(i) - \rho(i)]. \tag{17}$$

From Lemma 4 in Appendix D we have:

Proposition 3 *Let σ be a permutation different from the identity. Write the decomposition of σ into disjoint cycles as $\tau_1 \ldots \tau_t \sigma_1 \ldots \sigma_k$, using $\tau_1, \ldots, \tau_t$ to represent the disjoint cycles which are adjacent transpositions. Denote the lengths of $\sigma_1, \ldots, \sigma_k$ by $l_1, \ldots, l_k \geq 2$, respectively. Then*

$$\Delta(\sigma) \geq t + \sum_{j=1}^{k} l_j.$$

It follows that $\Delta(\sigma)$ is bounded below by a positive number so that $\mu(\rho)$ is the maximum mismatch. The "next best" maximum is given by the adjacent transposition, which has mismatch of 1.

Corollary 3 *Let $\sigma \in \mathcal{P}_n$ be an arbitrary permutation. Then $\mu(\rho\sigma) = \mu(\rho) - 1$ if and only if σ is an adjacent transposition.*

We conclude that the permutations $\rho\sigma$, $\sigma \in \mathcal{P}_\tau$ have the maximum mismatch of all permutations except the reversing permutation, ρ. Thus, for all $\sigma \in \mathcal{P}_\tau$, we have that $\mathbf{P}_{\rho\sigma}$ gives the "next best" minimum of (16).

5.2 Symmetry between attractive and repulsive solutions

As mentioned, we have found that there is a nice symmetry present in the solutions to the repulsive and attractive cases. This is formally stated in the following proposition which is proved in Appendix E. Let $\mathbf{r} = \mathbf{P}_\rho \mathbf{g}$. Note that because $\mathbf{P}_\rho$ is a reflection, $\mathbf{g} = \mathbf{P}_\rho \mathbf{r}$.

Proposition 4 *Let $\aleph = \{\alpha_\sigma^* \geq 0, \sigma \in \mathcal{P}_\tau\}$ such that $\sum_{\sigma \in \mathcal{P}_n} \alpha_\sigma^* = 1$. Then $\aleph$ is a solution of*

$$\min_{\bar{\alpha}} \sum_{\sigma \in \mathcal{P}_n} \alpha_\sigma \mathbf{r}^T \mathbf{P}_\sigma \mathbf{g}$$

if and only if $\aleph$ is a solution of

$$\max_{\bar{\alpha}} \sum_{\sigma \in \mathcal{P}_n} \alpha_\sigma \mathbf{g}^T \mathbf{P}_\sigma \mathbf{g}.$$

Reviewing, we have that the identity permutation is the best unconstrained solution to the symmetric problems:

$$\max_{\sigma \in \mathcal{P}_n} \mathbf{g}^T \mathbf{P}_\sigma \mathbf{g} \quad = \mathbf{g}^T \mathbf{g} \quad = \sum_{i=0}^{n-1} i^2, \tag{18}$$

and

$$\min_{\sigma \in \mathcal{P}_n} \mathbf{r}^T \mathbf{P}_\sigma \mathbf{g} \quad = \mathbf{r}^T \mathbf{g} \quad = \sum_{i=0}^{n-1} (n-1-i)i. \tag{19}$$

Continuing, let $\mathbf{P}_\tau$ represent any of the matrices computing an adjacent transposition. Then $\mathbf{P}_\tau$ is the solution to the symmetric problems:

$$\max_{\sigma \in \mathcal{P}_n - \{\mathbf{I}\}} \mathbf{g}^T \mathbf{P}_\sigma \mathbf{g} \quad = \mathbf{g}^T \mathbf{P}_\tau \mathbf{g} \quad = \mathbf{g}^T \mathbf{g} - 1, \tag{20}$$

and

$$\min_{\sigma \in \mathcal{P}_n - \{\mathbf{I}\}} \mathbf{r}^T \mathbf{P}_\sigma \mathbf{g} \quad = \mathbf{r}^T \mathbf{P}_\tau \mathbf{g} \quad = \mathbf{r}^T \mathbf{g} + 1. \tag{21}$$

Compare the two objective functions in these problems. If we replace $\mathbf{P}_\sigma$ in the minimization with $\mathbf{P}_\rho\mathbf{P}_\sigma$, we obtain

$$\mathbf{r}^T\mathbf{P}_\rho\mathbf{P}_\sigma\mathbf{g} = \mathbf{r}^T\mathbf{P}_\rho^T\mathbf{P}_\sigma\mathbf{g} = \mathbf{g}^T\mathbf{P}_\sigma\mathbf{g},$$

giving the two problems the same original objective function. Therefore, the solution to the minimization is just the solution to the maximization permuted by the reflection ρ.

It follows that if the ground state aura matrix for the attractive case is tridiagonal, then the ground state aura matrix for the repulsive case will be anti-tridiagonal. Given the same assumptions on the optimizations, the structure of the ground state matrix for one case will be the reversing reflection of the structure for the other case. In the same way, the sharpening that occurs along the diagonal for the attractive case will occur along the anti-diagonal for the repulsive case.

Combining this symmetry with Proposition 2, we can state the following key result for the structure of the repulsive isotropic auto-binomial GRF aura matrix:

Proposition 5 *For NM/n large enough compared with $4\pi\omega$ the ground state aura matrix of the repulsive isotropic auto-binomial GRF is anti-tridiagonal.*

Corollary 4 *The anti-trace of the ground state aura matrix of the repulsive isotropic auto-binomial GRF will increase linearly with respect to the number of graylevels. Let α_0 be the weight of the identity permutation. Then,*

$$\sum_{i=0}^{n-1} m(i, n-1-i) = \gamma\nu \sum_{i=0}^{n-1} \mathbf{m}(i, n-1-i) = \gamma\nu[n + (2\alpha_0 - 2)].$$

6 Structure of the auto-binomial aura matrix: anisotropic case

Here we consider the anisotropic case where β may vary both in sign and magnitude for different order neighborhoods.

6.1 Notation

It is helpful to define a *subneighborhood*, $\mathcal{N}_s^k \subset \mathcal{N}_s$ as the subset of neighbors having the same bonding parameter β_k. Each neighborhood can be written as a union of disjoint subneighborhoods,

$$\mathcal{N}_s = \bigcup_{k=1}^{K} \mathcal{N}_s^k, \quad \text{and} \quad \mathcal{N}_s^k \cap \mathcal{N}_s^l = \emptyset, \ \ \forall l \neq k, \ \ \forall s \in \mathcal{S}. \tag{22}$$

Letting the desired geometric primitive be the GRF subneighborhoods defined in (22) we have

$$m(g, g') = \sum_{k=1}^{K} m^k(g, g'), \tag{23}$$

where $m^k(g, g')$ is the aura measure over a two element symmetric neighborhood, $\mathcal{N}_s^k = \{s + d_k, \ s - d_k\}$. Forming an aura matrix over the subneighborhood k defines $\mathbf{A}^k = [m^k(g, g')]$ for $g, g' \in \Lambda$. In this case, $\mathbf{A}^k$ is just a symmetric co-occurrence matrix. From (23),

$$\mathbf{A} = \sum_{k=1}^{K} \mathbf{A}^k. \tag{24}$$

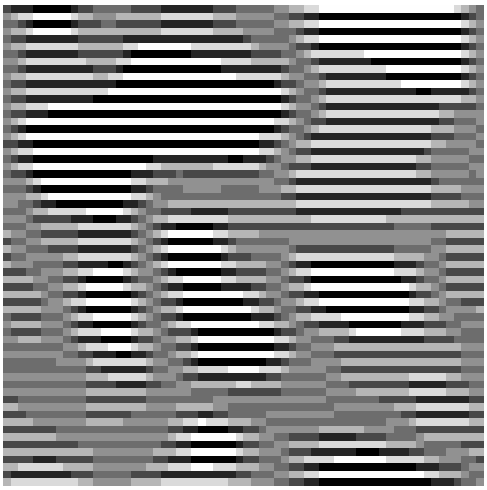

$$\mathbf{A}^1 = \begin{bmatrix} 926 & 98 & 0 & 0 & 0 & 0 & 0 & 0 \\ 98 & 772 & 154 & 0 & 0 & 0 & 0 & 0 \\ 0 & 154 & 690 & 180 & 0 & 0 & 0 & 0 \\ 0 & 0 & 180 & 678 & 166 & 0 & 0 & 0 \\ 0 & 0 & 0 & 166 & 680 & 178 & 0 & 0 \\ 0 & 0 & 0 & 0 & 178 & 690 & 156 & 0 \\ 0 & 0 & 0 & 0 & 0 & 156 & 774 & 94 \\ 0 & 0 & 0 & 0 & 0 & 0 & 94 & 930 \end{bmatrix}$$

$$\mathbf{A}^2 = \begin{bmatrix} 0 & 0 & 0 & 0 & 0 & 0 & 97 & 927 \\ 0 & 0 & 0 & 0 & 0 & 115 & 812 & 97 \\ 0 & 0 & 0 & 0 & 141 & 768 & 115 & 0 \\ 0 & 0 & 0 & 120 & 763 & 141 & 0 & 0 \\ 0 & 0 & 141 & 763 & 120 & 0 & 0 & 0 \\ 0 & 115 & 768 & 141 & 0 & 0 & 0 & 0 \\ 97 & 812 & 115 & 0 & 0 & 0 & 0 & 0 \\ 927 & 97 & 0 & 0 & 0 & 0 & 0 & 0 \end{bmatrix}$$

Figure 5: This 64×64 pattern was synthesized using a first order MRF with $n = 8$, $\beta_1 = 2$ (horizontal), and $\beta_2 = -2$ (vertical). The aura matrices for the two isotropic subneighborhoods are shown to illustrate their tridiagonal and anti-tridiagonal structure.

6.2 Formulation

For the anisotropic case it has previously been shown [4] that the expression in (5) becomes

$$\sum_{k=1}^{K} \beta_k \sum_{g,g' \in \Lambda} g g' m^k(g, g'). \tag{25}$$

In matrix form, the goal is to maximize

$$\sum_{k=1}^{K} \beta_k \mathbf{g}^T \mathbf{A}^k \mathbf{g}, \tag{26}$$

where $\mathbf{A}^k$ is the corresponding symmetric aura matrix of $m^k(g, g')$. Optimizing (26) corresponds to individually optimizing the $\beta_k \mathbf{g}^T \mathbf{A}^k \mathbf{g}$'s since they are over disjoint neighborhoods. Each of these terms then corresponds to an isotropic attractive or repulsive case.

For the first and second order GRF the subneighborhoods are "connected" in the sense that one can get from any neighbor to any other without leaving the neighborhood. In this case, or in the case of higher order neighborhoods and isotropy, the aura matrix is irreducible and the individual attractive or repulsive terms can be optimized as in the preceding sections. If the magnitudes of the bonding parameters, $|\beta_k|$, are constant for all k, and the conditions are such that Propositions 2 and 5 are valid, then the ground state aura matrices for each of the subneighborhoods will be either tridiagonal or anti-tridiagonal.

An example texture with aura matrices formed over subneighborhoods is shown in Figure 5. In this figure the patterns are not yet in a minimum energy configuration although the aura matrix structure is already present.

For the third and fourth order anisotropic GRF, if the anisotropy is such that one or more of the subneighborhoods are not connected, then the aura matrix is allowed to become reducible and the lower bound conditions need minor modification. We do not go into detail here, but give an example where this anisotropy will give different aura structure.

Example 3 *Suppose that β_6 is different from the other β_k, where $\mathcal{N}_s^6$ is the subneighborhood corresponding to the two horizontal third order elements. This subneighborhood is not connected since sites s and $s-(2,0)$ are separated by an element not in $\mathcal{N}_s^6$. Now consider a lattice with a pattern of binary vertical stripes, alternating every other pixel. Taking aura measures with respect to $\mathcal{N}_s^6$, this pattern will generate the diagonal aura matrix,*

$$\mathbf{A} = \begin{bmatrix} NM & 0 \\ 0 & NM \end{bmatrix}.$$

This matrix is allowed to be reducible since effectively the non-connected neighborhood breaks the lattice.

For $|\beta_k|$ varying, the terms with largest $|\beta_k|$ will become tridiagonal or anti-tridiagonal fastest following the interpretation of bonding parameters as temperature annealing rates [9]. The interaction of different rates in different directions leads to textural behavior that is much more difficult to predict, and often quite a bit more interesting visually.

7 Applications and implications

7.1 Restrictions on texture patterns

These new results on aura structure are significant for texture characterization. The ground state aura matrix characterizes the large scale behavior of the resulting pattern, and the sharpening process introduces zeros in the aura matrix which indicate that certain colors will not exist as neighbors in the pattern.

For the case of tridiagonal structure and $n > 2$, elements of $\mathbf{A}$ that satisfy $|g - g'| > 1$ will be zero. This implies that textures in the ground states cannot have any mixing among graylevels g, g' when $|g - g'| > 1$. For the case of anti-tridiagonal structure, textures in the ground states cannot have any mixing between graylevels g and $n - 1 - g'$ when $|g - g'| > 1$. These are serious restrictions, especially during *a posteriori* maximization where the model is ideally sampled in its ground state.

For anisotropic models, when the ground state aura matrix consists of a linear combination of tridiagonal and anti-tridiagonal matrices and $n \geq 5$, then the aura measures $m(g, g')$ and $m(g, n-1-g')$ with $|g - g'| > 1$ will be forced to be zero. This can seriously limit texture patterns formed by energy minimization of GRF's. Patterns are prohibited from having colors g, g' interact, when g and g' are not indices of either a tridiagonal or an anti-tridiagonal element.

Moreover, the sharpening process which happens on the way to the ground state gradually restricts the space of feasible textures. Even as the matrices are *becoming* tridiagonal or anti-tridiagonal (i.e., not yet in their ground states) their intermediate banded structures imply which large classes of configurations are exceedingly unlikely to occur. This bandedness has also been related to the temperature of the model [12] so that the temperature can be used to guide these stages of pattern formation.

We have seen that the ground state structure results in a global pattern unlike the small scale random patterns usually associated with GRF texture models. Note that the ground state pattern is not unique since the assumption of the periodic lattice implies that the same pattern could occur in NM different positions.

Note also that the method developed to analyze the ground states of the auto-binomial model can be generalized to deal with *any* model having a separable interaction potential of the form $V(g,g') = F(g)H(g')$, where F and H are two strictly monotonic functions of the pattern graylevels. However, in some special cases where separability and monotonicity are both lacking, Birkhof's decomposition would still give us insight into the structure of the model ground states. We illustrate this fact in the next paragraph in which we deal with another important class of Gibbs models, the Potts model.

7.2 Application to the Potts texture model

The Potts model (which is employed, although not by this name in [3, 13]) can also be analyzed using the methodology and assumptions of this paper. The pairwise interaction potential for the isotropic homogeneous Potts field is $V(g,g') = 2\delta_{gg'} - 1$, where $\delta_{gg'}$ is the Kronecker delta symbol [14]. After substituting this potential into the energy expression of (4), the optimization problem for the Potts model is

$$\max_{\mathbf{x}\in\mathbf{\Omega}} \beta \left(\sum_{g\in\Lambda} m(g,g) - 2 \sum_{g<g'} m(g,g') \right). \tag{27}$$

Observe that (27) does not distinguish between graylevels other than if they are the same or different. Let $\mathbf{w}$ be an n-vector of 1's, and let $\mathbf{D}$ be a diagonal $n \times n$ matrix of the self-aura measures. Then the objective function to be maximized is alternatively written as

$$\beta\, [3\mathbf{w}^T\mathbf{D}\mathbf{w} - 2\mathbf{w}^T\mathbf{A}\mathbf{w}]. \tag{28}$$

Attractive case ($\beta > 0$): We want to minimize $\mathbf{w}^T\mathbf{A}\mathbf{w}$ and maximize $\mathbf{w}^T\mathbf{D}\mathbf{w}$. Clearly the aura matrix will try to become diagonal, subsequently maximizing the self-aura measures.

Observe that this is the same boundary minimization problem as the auto-binomial case without the ordering influence of the different graylevels. In other words, even if the aura matrix $\mathbf{A}$ is normalized and decomposed into permutations all the permutations would have the same effect on the energy. Consequently, no permutations are favored for the cross-aura measures. The resulting aura matrix structure is diagonally dominant with uniformly distributed off-diagonal elements. Notice that if the histogram is not constrained for the Potts energy then the lattice will become unicolor.

Repulsive case ($\beta < 0$): The goal is to maximize $\mathbf{w}^T\mathbf{A}\mathbf{w}$ and minimize $\mathbf{w}^T\mathbf{D}\mathbf{w}$. For this case $\mathbf{w}^T\mathbf{D}\mathbf{w}$ can usually be driven to zero without violating the irreducibility of the aura matrix. The resulting aura matrix structure has zeros along the main diagonal with the remainder of the values uniformly distributed along the off-diagonals. It follows that no two elements of the same color can be neighbors in the ground state. Again, this is a very serious restriction for a texture model [4].

Anisotropic case: The anisotropic Potts case can be obtained from the isotropic cases by examining the energy minimization over the subneighborhoods. Let $\mathbf{D}^k$ be a diagonal $n \times n$ matrix of the self-aura measures over the subneighborhood $\mathcal{N}_s^k$. Then the objective function to be maximized is

$$\sum_{k=1}^{K} \beta_k [3\mathbf{w}^T\mathbf{D}^k\mathbf{w} - 2\mathbf{w}^T\mathbf{A}^k\mathbf{w}]. \tag{29}$$

[4] However, this result should not surprise a reader familiar with the connections between graph coloring and the Potts model [14].

Again, because of the linearity of the energy and the disjointness of the subneighborhoods, the positive and negative terms can be optimized individually. For each direction k, if $\beta_k > 0$ then the synthesis will try to maximize the elements along the diagonal and if $\beta_k < 0$ then it will try to zero the elements along the diagonal.

7.3 Implications for co-occurrence structure

In surveys of texture analysis, Haralick [15], Wechsler [16], and Van Gool *et. al.* [17] discuss both co-occurrence matrices and random field methods. Van Gool *et. al.* basically summarize the understanding of the structure of co-occurrence matrices by noting that if the displacement is small relative to the texture coarseness the matrix values cluster near the main diagonal, while for larger displacements, the values are more spread out. None of the surveys recognize any connection between GRF's and co-occurrences.

We believe that the aura matrix establishes the first link between a texture model and the structure of its co-occurrence matrix. The GRF models in this paper are completely characterized by the aura matrix; hence, they are also completely characterized by the corresponding set of co-occurrences. Since co-occurrence and GRF aura matrices have only nonnegative elements and the aura matrix is a sum of co-occurrence matrices, then a zero in the aura matrix implies corresponding zeros in the co-occurrence matrices. By showing there is structure in the GRF ground state aura matrices, we have shown there is corresponding structure in the co-occurrence matrices.

8 Conclusions

We have shown that under certain assumptions the structure of the aura and co-occurrence matrices is either tridiagonal or anti-tridiagonal for the ground state isotropic, auto-binomial GRF. Consequently, the theory presented here accounts for the experimental behavior observed during texture formation in earlier publications [4, 9]. For the anisotropic, auto-binomial GRF, the aura matrix is formed by linearly combining the constituent isotropic matrices. Thus, its ground state is a combination of the tridiagonal and anti-tridiagonal structures. For five or more graylevels, we have shown zeros will appear in the ground state matrices; these correspond to restrictions on miscibility between different colors. Such restrictions severely limit the kinds of texture patterns that occur when the Gibbs energy is minimized. The study of the Potts model has also revealed stringent restrictions on the type of ground states. These restrictions should be understood before modeling images with Gibbs random fields. Indeed, the Bayesian approach to image processing and low level vision is typically based on the choice of an *a priori* model and the maximization, often by simulated annealing, of an *a posteriori* probability. Our results, which concern the *a priori* model, imply that one might be surprised by what is at the end of the maximization.

9 Acknowledgments

We would like to acknowledge the helpful support and encouragement of Alex P. Pentland and John Wyatt, Jr.. Thanks also to the anonymous reviewers, Trevor Darrell, and Alex Sherstinsky for their comments which helped improve the clarity of this paper.

A Permutations, cycles, transpositions

A *permutation* of the vector $\mathbf{g} = [0, 1, \ldots, n-1]^T$ gives a rearrangement of its elements. Every permutation can be represented by a *permutation matrix*: an orthogonal matrix having in every row and column exactly one nonzero coefficient equal to 1. The following examples illustrate the use of permutation matrices to rearrange the vector $\mathbf{g}$.

Example 4 *Suppose that we form the product of the* permutation matrix $\mathbf{P}_{\sigma_1}$ *with* $\mathbf{g}$,

$$\mathbf{P}_{\sigma_1}\mathbf{g} = \begin{bmatrix} 0 & 0 & 0 & 1 & 0 \\ 1 & 0 & 0 & 0 & 0 \\ 0 & 0 & 1 & 0 & 0 \\ 0 & 1 & 0 & 0 & 0 \\ 0 & 0 & 0 & 0 & 1 \end{bmatrix} \begin{bmatrix} 0 \\ 1 \\ 2 \\ 3 \\ 4 \end{bmatrix} = \begin{bmatrix} 3 \\ 0 \\ 2 \\ 1 \\ 4 \end{bmatrix}.$$

We say that this is equivalent to permuting the vector $\mathbf{g} = [0, 1, 2, 3, 4]^T$ by the *cycle* $\sigma_1 = (3, 1, 0)$. It is a well known result in algebra [11] that any permutation can be written as a product of its disjoint cycles. The permutation σ_1 consists of only one cycle of length 3. Note that using the cycle notation, $(3, 1, 0) = (0, 3, 1) = (1, 0, 3)$.

Example 5 The permutation

$$\mathbf{P}_{\sigma_2} = \begin{bmatrix} 0 & 0 & 1 & 0 & 0 \\ 0 & 1 & 0 & 0 & 0 \\ 1 & 0 & 0 & 0 & 0 \\ 0 & 0 & 0 & 0 & 1 \\ 0 & 0 & 0 & 1 & 0 \end{bmatrix}$$

can be written as the product of its disjoint cycles,

$$\sigma_2 = (0, 2)(3, 4).$$

In Example 5 the cycles are called *transpositions* because they have length 2. The cycle $(3, 4)$ is also an *adjacent transposition* since it transposes two elements $j, j+1$.

If the cycles are not disjoint then they are applied from right to left.

Example 6 *Let* σ_1 *and* σ_2 *be the same as in Examples 4 and 5. Applying the new permutation* $\sigma_3 = \sigma_2\sigma_1$ *to* $\mathbf{g}$ *yields*

$$\mathbf{P}_{\sigma_2}\mathbf{P}_{\sigma_1}\mathbf{g} \quad = \quad \mathbf{P}_{\sigma_2}[3, 0, 2, 1, 4]^T = [2, 0, 3, 4, 1]^T.$$

B Proof of Proposition 1

The following three lemmas are used to prove Proposition 1.

Lemma 1 *Let* $\sigma \in \mathcal{P}_\tau$ *be an adjacent transposition. Then* $\mu(\sigma) = 1$.

Proof: Assume that σ exchanges the adjacent elements $j, j+1 \in \Lambda$. Then its mismatch

$$\begin{aligned}\mu(\sigma) &= \sum_{i=0}^{n-1}[i^2 - i\sigma(i)] \\ &= \sum_{i\in\{j,j+1\}}[i^2 - i\sigma(i)] + \sum_{i\in\Lambda-\{j,j+1\}}[i^2 - i\sigma(i)] \\ &= j^2 - j(j+1) + (j+1)^2 - (j+1)j = (j-(j+1))^2 = 1.\end{aligned}$$

■

Is there any other permutation that has a mismatch this small? The answer is no, and comes from the next two lemmas. The first lemma gives a lower bound on the mismatch associated with a cycle that is not an adjacent transposition. The second shows that the mismatch of a permutation will be the sum of the mismatches of its cycles.

Lemma 2 *Let $\sigma \in \mathcal{P}_n - \mathcal{P}_\tau^*$ be a cycle of length l. Then*

$$\mu(\sigma) \geq l. \tag{30}$$

Proof: The proof is by induction on the length. First, assume that σ has $l = 2$ but is not adjacent. Let $j, k \in \Lambda$, with $|j-k| \geq 2$. Then

$$\begin{aligned}\mu(\sigma) &= \sum_{i=0}^{n-1}[i^2 - i\sigma(i)] \\ &= \sum_{i\in\{j,k\}}[i^2 - i\sigma(i)] + \sum_{i\in\Lambda-\{j,k\}}[i^2 - i\sigma(i)] \\ &= j^2 - jk + k^2 - kj = (j-k)^2 \geq 4.\end{aligned}$$

Next, consider the two possible arrangements for cycles having $l = 3$: $\sigma_1 = (i,j,k)$ and $\sigma_2 = (i,k,j)$. Then

$$\begin{aligned}\mu(\sigma_1) &= i^2 - ij + j^2 - jk + k^2 - ki \\ &= \frac{1}{2}[(i-j)^2 + (j-k)^2 + (k-i)^2] \geq 3,\end{aligned}$$

and

$$\begin{aligned}\mu(\sigma_2) &= i^2 - ik + k^2 - kj + j^2 - ji \\ &= \frac{1}{2}[(i-k)^2 + (k-j)^2 + (j-i)^2] \geq 3,\end{aligned}$$

so (30) is true for $l = 2, 3$.

Finally, assume that (30) is true for length $l \geq 3$, and show that it is true for length $l+1$. Let σ have length $l+1$. We can always shift the cycle until its maximum element is written in the last position, $\sigma = (i_0, i_1, \ldots, i_l)$, where $i_l = \max\{i_0, i_1, \ldots, i_l\}$. Now, form the l-length cycle, $\sigma' = (i_0, i_1, \ldots, i_{l-1})$. By the induction assumption, $\mu(\sigma') \geq l$. But

$$\mu(\sigma) = \sum_{j=0}^{l}[i_j^2 - i_j\sigma(i_j)]$$

$$
\begin{aligned}
&= \sum_{j=0}^{l-2}[i_j^2 - i_j\sigma(i_j)] + [i_{l-1}^2 - i_{l-1}i_l] + [i_l^2 - i_l i_0] \\
&= \sum_{j=0}^{l-2}[i_j^2 - i_j\sigma(i_j)] + [i_{l-1}^2 - i_{l-1}i_0] + i_{l-1}i_0 - i_{l-1}i_l + [i_l^2 - i_l i_0] \\
&= \sum_{j=0}^{l-1}[i_j^2 - i_j\sigma'(i_j)] + i_l^2 - i_l i_0 - i_{l-1}i_l + i_{l-1}i_0 \\
&= \mu(\sigma') + (i_l - i_{l-1})(i_l - i_0) \;\geq\; l+2 \;>\; l+1.
\end{aligned}
$$

■

Lemma 3 *Let $\sigma = \sigma_1 \ldots \sigma_k$ be the decomposition of the permutation σ into its disjoint cycles. Then*

$$\mu(\sigma) = \sum_{j=1}^{k} \mu(\sigma_j).$$

Proof: Let Λ_j be the set of elements permuted by cycle σ_j. Since the cycles are disjoint the Λ_j form a partition of Λ. When $i \in \Lambda_j$, $\sigma(i) = \sigma_j(i)$ and when $i \in \Lambda - \Lambda_j$, $\sigma(i) = i$. Thus,

$$
\begin{aligned}
\mu(\sigma) &= \sum_{i\in\Lambda}[i^2 - i\sigma(i)] \;=\; \sum_{j=1}^{k}\sum_{i\in\Lambda_j}[i^2 - i\sigma_j(i)] \\
&= \sum_{j=1}^{k}\sum_{i\in\Lambda}[i^2 - i\sigma_j(i)] \;=\; \sum_{j=1}^{k}\mu(\sigma_j).
\end{aligned}
$$

■

The proof of Proposition 1 is completed as follows. From Lemma 3, the bound on the permutation $\mu(\sigma)$ will come from the sum of the bounds on its disjoint cycles. From Lemma 1, each of the t adjacent transpositions contributes a mismatch of 1, and from Lemma 2, the other k cycles contribute mismatches which are at least their lengths, l_j.

C Proof of Corollary 2

Proof: From the decomposition of the ground state miscibility matrix we have,

$$\mathbf{M} = \alpha_0\mathbf{I} + \hat{\alpha}\sum_{\sigma\in\mathcal{P}_\tau}\mathbf{P}_\sigma.$$

Each of the $n-1$ adjacent permutation matrices has $n-2$ elements remaining on the diagonal. Summing, and using the constraint on the coefficients, its trace is

$$
\begin{aligned}
\sum_{i=0}^{n-1}\mathbf{m}(i,i) &= n\alpha_0 + (n-2)(n-1)\hat{\alpha} \\
&= n\alpha_0 + (n-2)(1-\alpha_0) = n + 2\alpha_0 - 2.
\end{aligned}
$$

The aura matrix trace follows by scaling the miscibility matrix entries. ■

D Proof of Proposition 3

Lemma 4 *Let $\sigma \in \mathcal{P}_n$. Then $\Delta(\sigma) = \mu(\sigma)$.*

Proof:

$$\begin{aligned}\Delta(\sigma) &= \sum_{i=0}^{n-1} i[\rho\sigma(i) - \rho(i)] = \sum_{i=0}^{n-1} i[n-1-\sigma(i)-(n-1-i)] \\ &= \sum_{i=0}^{n-1} i[i-\sigma(i))] = \mu(\sigma).\end{aligned}$$

■

E Proof of Proposition 4

Proof: Suppose $\aleph$ is a solution of

$$\max_{\bar{\alpha}} \sum_{\sigma \in \mathcal{P}_n} \alpha_\sigma \mathbf{g}^T \mathbf{P}_\sigma \mathbf{g},$$

then it also solves the problem

$$\min_{\bar{\alpha}} \sum_{\sigma \in \mathcal{P}_n} \alpha_\sigma \left[\mathbf{g}^T \mathbf{g} - \mathbf{g}^T \mathbf{P}_\sigma \mathbf{g}\right],$$

which is by definition and by Lemma 4,

$$\min_{\bar{\alpha}} \sum_{\sigma \in \mathcal{P}_n} \alpha_\sigma \mu(\sigma) = \min_{\bar{\alpha}} \sum_{\sigma \in \mathcal{P}_n} \alpha_\sigma \Delta(\sigma).$$

The right hand minimization problem is equivalent to

$$\min_{\bar{\alpha}} \sum_{\sigma \in \mathcal{P}_n} \alpha_\sigma \left[\mathbf{g}^T \mathbf{P}_\rho \mathbf{P}_\sigma \mathbf{g} - \mathbf{g}^T \mathbf{P}_\rho \mathbf{g}\right],$$

or noting that $\mathbf{P}_\rho^T = \mathbf{P}_\rho$ and $\mathbf{r} = \mathbf{P}_\rho \mathbf{g}$,

$$\min_{\bar{\alpha}} \sum_{\sigma \in \mathcal{P}_n} \alpha_\sigma \left[\mathbf{r}^T \mathbf{P}_\sigma \mathbf{g} - \mathbf{g}^T \mathbf{r}\right].$$

This problem is equivalent to the maximization,

$$\max_{\bar{\alpha}} \sum_{\sigma \in \mathcal{P}_n} \alpha_\sigma \left[\mathbf{g}^T \mathbf{r} - \mathbf{r}^T \mathbf{P}_\sigma \mathbf{g}\right],$$

which is solved by $\aleph$ if and only if the following is solved by $\aleph$:

$$\min_{\bar{\alpha}} \sum_{\sigma \in \mathcal{P}_n} \alpha_\sigma \mathbf{r}^T \mathbf{P}_\sigma \mathbf{g}.$$

■

References

[1] J. Besag, "Spatial interaction and the statistical analysis of lattice systems (with discussion)," *J. Roy. Stat. Soc., Ser. B*, vol. 36, pp. 192–236, 1974.

[2] G. R. Cross and A. K. Jain, "Markov random field texture models," *IEEE T. Patt. Analy. and Mach. Intell.*, vol. PAMI-5, no. 1, pp. 25–39, 1983.

[3] S. Geman and D. Geman, "Stochastic relaxation, Gibbs distributions, and the Bayesian restoration of images," *IEEE T. Patt. Analy. and Mach. Intell.*, vol. PAMI-6, no. 6, pp. 721–741, 1984.

[4] I. M. Elfadel and R. W. Picard, "Miscibility matrices explain the behavior of grayscale textures generated by Gibbs random fields," in *Proc. SPIE Conf. on Intell. Robots and Comp. Vis.*, vol. 1381, (Boston, MA), pp. 524–535, Nov. 1990.

[5] S. W. Zucker and D. Terzopoulos, "Finding structure in co-occurrence matrices for texture analysis," *Comp. Vis., Graph., and Img. Proc.*, vol. 12, pp. 286–308, 1980.

[6] G. R. Cross, *Markov Random Field Texture Models*. PhD thesis, Michigan State Univ., 1980.

[7] L. Garand and J. A. Weinman, "A structural-stochastic model for the analysis and synthesis of cloud images," *J. of Climate and Appl. Meteorology*, vol. 25, pp. 1052–1068, 1986.

[8] I. M. Elfadel and R. W. Picard, "Auras part I: Theory and relation to morphology and co-occurrence," tech. rep., MIT Media Lab, Vision and Modeling TR #149, Feb. 1991.

[9] R. W. Picard, I. M. Elfadel, and A. P. Pentland, "Markov/Gibbs texture modeling: Aura matrices and temperature effects," in *Proc. IEEE Conf. on Computer Vision and Pattern Recognition*, (Maui, HI), pp. 371–377, June 1991.

[10] G. Strang, *Introduction to Applied Mathematics*. Cambridge, MA: Wellesley-Cambridge Press, 1986.

[11] I. M. Herstein, *Topics in Algebra*. New York: Wiley, 1975.

[12] R. W. Picard and A. P. Pentland, "Markov/Gibbs image modeling: Temperature and texture," in *Proc. SPIE Conf. on Intell. Robots and Comp. Vis.*, vol. 1607, (Boston, MA), pp. 15–26, Nov. 1991.

[13] H. Derin and H. Elliott, "Modeling and segmentation of noisy and textured images using Gibbs random fields," *IEEE T. Patt. Analy. and Mach. Intell.*, vol. PAMI-9, no. 1, pp. 39–55, 1987.

[14] R. J. Baxter, *Exactly Solved Models In Statistical Mechanics*. London: Academic Press, Inc., 1982.

[15] R. Haralick, "Statistical and structural approaches to texture," *Proc. IEEE*, vol. 67, pp. 786–804, May 1979.

[16] H. Wechsler, "Texture analysis – a survey," *Signal Processing*, vol. 2, no. 3, pp. 271–282, 1980.

[17] L. Van Gool, P. Dewaele, and A. Oosterlinck, "Texture analysis anno 1983," *Computer Vision, Graphics, and Image Processing*, vol. 29, pp. 336–357, 1985.